BILINGUAL PUBLISHING GROUP

Journal of Atmospheric Science Research
https://journals.bilpubgroup.com/index.php/jasr

ARTICLE

Variation of Dynamical Parameters with Upper Tropospheric Potential Vorticity in Tropical Cyclone over the North Indian Ocean Using WRF Model

***A.H.M. Fazla Rabbi*[1*], *Ishtiaque M. Syed*[1], *Md. Abdullah Elias Akhter*[2], *M A K Mallik*[3]**

[1] *Department of Physics, University of Dhaka, Dhaka, 1000, Bangladesh*
[2] *Department of Physics, Khulna University of Engineering and Technology, Khulna, 9208, Bangladesh*
[3] *Bangladesh Meteorological Department, Agargaon, Dhaka, 1207, Bangladesh*

ABSTRACT

Meteorologists are experiencing many challenges in the reliable forecasting of the track and intensity of tropical cyclones (TC). Uses of the potential vorticity (PV) technique will enrich the current forecasting system. The use of PV analysis of TC intensification over the North Indian Ocean (NIO) is rare. In this study, the authors analyze the behaviour of upper-level PV with dynamic parameters of TCs over NIO. The authors used NCEP FNL reanalysis 1 × 1 degree data as input in WRF model version 4.0.3 with one-way nesting between the parent and child domains. The authors used a coupling of the Kain-Fritsch (new Eta) scheme and the WSM 6-class graupel scheme as cumulus and microphysics options to run the model. The authors found that at least one potential vorticity unit (PVU) (1 PVU = 10^{-6} $m^2s^{-1}KKg^{-1}$) upper PV is required to maintain the intensification of TC. Larger upper PV accelerates the fall of central pressure. The high value of upper PV yields the intensification of TC. The wind shear and upper PV exhibited almost identical temporal evolution. Upper PV cannot intensify the TCs at negative wind shear and shear above the threshold value of 12 ms^{-1}. The upper PV and geopotential heights of 500 hPa change mutually in opposite trends. The upper PV calculated by the model is comparable to that of ECMWF results. Therefore, the findings of this study are admissible.

Keywords: Dynamic; Vorticity; Geopotential; WRF; Tropical and intensification

*CORRESPONDING AUTHOR:
A.H.M. Fazla Rabbi, Department of Physics, University of Dhaka, Dhaka, 1000, Bangladesh; Email: rabbiphy@gmail.com

ARTICLE INFO
Received: 10 May 2023 | Revised: 11 July 2023 | Accepted: 18 July 2023 | Published Online: 25 July 2023
DOI: https://doi.org/10.30564/jasr.v6i3.5717

CITATION
Fazla Rabbi, A.H.M., Syed, I.M., Akhter, M.A.E., et al., 2023. Variation of Dynamical Parameters with Upper Tropospheric Potential Vorticity in Tropical Cyclone over the North Indian Ocean using WRF Model. Journal of Atmospheric Science Research. 6(3): 20-29. DOI: https://doi.org/10.30564/jasr.v6i3.5717

1. Introduction

A tropical cyclone maintains its life cycle by the energy that originates from the warmed moisture of the ocean surface. This warmed moisture releases latent heat in the eye wall of TC. The low-level inflow of moisture content wind and its spiraling upward motion flare up the PV of TC. The analysis of PV is a promising technique in meteorology. The facts from that analysis make the tropical cyclones (TC) more perceptible. Incorporating the concept of PV structure in current meteorology, forecasters and researchers may have many advantages in synoptic-scale forecasting of atmospheric events. Superposition of the upper PV anomaly and low-level centre nourish the TC's intensification [1].

The formation of a hollow tower of PV structure also favours the rapid intensification of TC. On the other hand, the detritions of PV structure decline the TC intensification [2,3]. Upper-level PV anomalies are crucial for storm motion. The impact of PV anomalies on the storm motions depends on the upper-tropospheric PV characteristics and corresponding locations of the vortex [4,5].

Upper-level PV streamer and middle-low-level PV anomalies exist in the genesis stage of the Mediterranean cyclone. Also, an acute PV tower stretches from the upper troposphere to the lower stratosphere found in one of the Mediterranean cyclones [6]. Convective heating gives rise to positive potential vorticity in and outside the ring area of TC. Positive potential vorticity at the matured stage of TC is crucial to maintaining the ring structure and the feedback process [7].

A narrow tower of maximum potential vorticity exists on the inner edge of the eyewall cloud of a matured Hurricane. In such a structure, potential vorticity can reach several hundred PV units [8]. Higher PV within the stratiform regions is the prime PV source for the intensification of TC [9]. Latent heat release originates the low-level PV. Vertical advection of latent heat broadens the low-level PV and stretches it up to the upper level [10,11].

The term annular heating function is suitable to describe the distribution of latent heat release in the eye wall of TC. Vertical advection of annular heating is more realistic than the descending of isentropes. The PV maximum exists adjacent to the radius of maximum heating [12]. The entropy difference between the air and sea allows more and more energy to TC from the underneath sea surface. The PV mixing from the eye wall to the inner core limits the entropy difference between the air-sea surfaces and prevents the TC intensity [13]. Heating the outer spiral rain bands declines the intensity of TC and increases the size of TC. Cooling the outer rain bands favour the strength and tightly packed inner core of TC [14].

Outward distribution of high PV from the inner core of TC raises the local isentropic surfaces and establishes a cold dome stretching from the mid to lower troposphere [15]. A considerable generation of PV in the rain band area is an indispensable factor for the secondary eyewalls in TC [16]. Concentric and compact eyewalls approaching smaller sizes exist in the intense stage of TC. Circular bands of maximum PV establish in the corresponding maximum vertical motions area of the eyewall and have powerful interaction with eyewall convection [17].

500 hPa level is considered half of the earth's troposphere. Below this level, the wind flow has the same direction. Hence atmospheric events at this level play a vital role in the genesis and intensification of TC. Fall of geopotential height cause turbulent weather phenomena. This atmospheric condition favour instability and convection of cloud accompanied by heavy rainfall [18]. The variation of geopotential heights of 500 hPa level may impact the dynamics of climate change via the change in circulation pattern [19].

The aim of this study is to find out the influence of upper PV on the dynamic parameters of TC over the NIO.

2. Synoptic study of TCs

A) **Ashoba:** A low-level cyclonic circulation developed over southeast AS on 5th June 2015 due to the southwest monsoon onset over Kerala. By the morning of 6th June, it moved northwards and concentrated into an LPA over the southeast and

adjoining east-central AS. Sufficient SST, low-level convergence, upper-level divergence, low-level relative vorticity and weak to moderate vertical wind shear favoured the concentration of the system into depression at 0300 UTC of 7th June over east-central AS. The system moved north-northwestward and intensified into DD at 0000 UTC on 8th June. At 0300 UTC on 8th June, the system turned into CS Ashoba. It continued its north-northwestward movement till 0900 UTC on 8th June and then moved northwards till 0600 UTC on 9th June. After that, it moved west-northwards till 0600 UTC on 10th June and west-southwestwards till 0000 UTC on 11th June. Later, the system moved westwards slowly and switched into DD at 1800 UTC on the 11th of June. It weakened into a depression at 0000 UTC on 12th June and WML over the northwest AS and adjoining Oman coast at 1200 UTC on 12th June.

B) **Titli:** A Very Severe Cyclonic Storm (VSCS) Titli formed over southeast BoB is considered in our present study. This system originated from the low-pressure area (LPA) over southeast BoB and adjoining north Andaman Sea at 0300 UTC on 7th October 2018. It intensified into a well-marked low (WML) at 1200 UTC on 7th October 2018. It then concentrated into a depression (D) over east-central BoB at 0300 UTC on 8th October 2018. The system advanced west north-westward and intensified into a deep depression (DD) over east central BoB at about 1800 UTC on 8th October 2018 and further intensified into cyclonic storm (CS) Titli at around 0600 UTC on 9th October 2018. It intensified into a severe cyclonic storm (SCS) at 2100 UTC on 9th October 2018 during its north-westward movement. Then it moved north-northwestwards at 0600 UTC on 10th October 2018 and evolved as a very severe cyclonic storm (VSCS), the highest intensification stage of its life cycle. It crossed north Andhra Pradesh and south Odisha coasts near Palasa at 18.8° N and 84.5° E during 2300 UTC on 10th October and 0000 UTC on 11th October 2018 as a VSCS. During this crossing, the wind speed was 140-150 Kmph gusting to 165 Kmph. It then moved north-westward and weakened into an SCS around 0600 UTC on 11th October and into a cyclonic storm (CS) around 1200 UTC of the same day. It turned into a DD over south Odisha at midnight (1800 UTC) on 11th October 2018.

C) **Mekunu:** A cyclonic circulation over Lakshadweep and its neighbourhood caused the formation of LPA over southeast AS at 0300 UTC on 20th May 2018. At 0000 UTC of 21st May, it appeared as a WML over the southwest and adjoining southeast AS. The Madden Julian Oscillation of phase 2 at 0300 UTC on 21st May favoured the cyclogenesis and further intensification. The environmental conditions such as SST, low-level relative vorticity, low-level relative convergence, upper-level divergence and vertical wind shear maintained the required value to sustain the cyclogenesis. This environmental condition continued till 1200 UTC on 21st May and the system concentrated as the depression over southwest and adjoining southeast AS. Weak to moderate vertical wind shear and successive increments of, low-level relative vorticity, low-level relative convergence, and upper-level divergence caused the further intensification of the system to DD at 0300 UTC on 22nd May. The system intensified as CS Mekunu at 1200 UTC on the 22nd, SCS at 0300 UTC, VSCS at 0900 UTC on the 23rd of May and reached its peak intensity ESCS at 0300 UTC on the 24th of May, 2018. It crossed the south Oman coast as ESCS between 1830 and 1930 UTC on 25th May 2018. By 0300 UTC on 27th May 2018, this system weakened into a WML over Saudi Arabia and adjoining areas of Oman & Yemen.

D) **Amphan:** A remnant of LPA over the south Andaman Sea and adjoining southeast BOB from 6th to 12th May 2020 influenced the formation of another fresh LPA over southeast BOB and adjacent south Andaman Sea at 0300 UTC on 13th May 2020. It became WML over southeast BOB and its neighbourhood at 0300 UTC on 14th May. Under favourable conditions, it turned into a depression (D) at 0000UTC and concentrated into DD at 0900UTC on 16th May over southeast BOB. After the north-northwestward movement, it developed as CS Amphan at 1200 UTC on 16th May 2020 over southeast BOB. It further intensified into a Severe Cyclonic Storm

(SCS) at 0300UTC, Very Severe Cyclonic Storm (VSCS) at 0900 UTC and Extremely Severe Cyclonic Storm (ESCS) at 2100 UTC on 17th May. At 0600 UTC on 18th May 2020, it intensified into Supper Cyclonic Storm (SuCS). This stage lasted about 24 hours and weakened into ESCS over west-central BOB at 0600 UTC on 19th May. It crossed the West Bengal-Bangladesh coasts as a VSCS across Sundarbans during 1000-1200 UTC on 20th May with a maximum sustained wind speed of 155-165 Kmph.

3. Data and methods

The WRF model version 4.0.3 is used to simulate the dynamic features of TCs. The model runs took place following the best track position and status provided by the satellite observations of the Indian Meteorological Department (IMD) (**Table 1**). We used NCEP FNL reanalysis 1 × 1 degree data in the simulations. A one-way nesting method is used to set up the domains. The horizontal resolutions of parent and child domains were 21 and 7 km. Arakawa C-grid staggering was used as grid distribution. Mercator map used in projection for the model run. A coupling of the Kain-Fritsch (new Eta) scheme and WSM6-class graupel scheme as cumulus and microphysics option was used in the runs. Ertel's hydrostatic potential vorticity equation $PV = -g(\zeta_\Theta + f)\frac{\partial \Theta}{\partial p}$ used in this study, where ζ_Θ is the relative vorticity, f is the coriolis parameter, g is the gravitational acceleration, Θ is the potential temperature and p is the pressure. This study was accomplished using the outputs of the inner domain of 10° × 10° **areal extent**. We calculated maximum PV at 200 hPa level, wind speed at 850 hPa, central pressure and vertical wind shear between 850 and 200 hPa within the corresponding area of the inner domain. We also calculated the geopotential height GPH = $\frac{\Phi}{g_0}$, where $\Phi = gz$ the geopotential and g_0 is the standard value of gravitational acceleration. We visualized the model outputs using the GrADS software. The model outputs compared with the ECMWF Reanalysis 5th Generation (ERA5) hourly data of 0.25° × 0.25° horizontal resolution.

4. Results and discussion

4.1 Temporal evolution of upper potential vorticity

The analysis of PV for forecasting the genesis and intensification of TC is very significant in current meteorology. The temporal evolution of upper tropospheric PV may give us important insights into the intensification of TC. Therefore, the facts and findings from the PV analysis will enrich the present forecasting system. At least 1 PVU is required to sustain the TC intensification shown in the PV's time evolution for the matured TCs. The time evolution of PV in the model and ECMWF is comparable (**Figure 1**). For Amphan and Mekunu, the model and ECMWF have calculated PVs that are close to each

Table 1. Schedule of WRF model run following IMD satellite-based best track positions.

Event Name	Location	Model run start at	Model run end at	Initial condition	End condition	Maximum intensity during model run
Ashoba	AS	0600UTC of June 08, 2015	0600UTC of June 11, 2015	CS	CS	CS
Titli	BOB	0600UTC of October 09, 2018	0600UTC of October 12, 2018	CS	DD	VSCS
Mekunu	AS	1200UTC of May 22, 2018	1200UTC of May 25, 2018	CS	ESCS	ESCS
Amphan	BOB	1200UTC of May 16, 2020	1200UTC of May 19, 2020	CS	ESCS	SuCS

*DD: Deep Depression, CS: Cyclonic Storm, VSCS: Very Severe Cyclonic Storm, ESCS: Extremely Severe Cyclonic Storm, SuCS: Supper Cyclonic Storm.

other most of the time. The ups and downs of upper PVs have a similar fashion in all TCs. In the peaks of upper PV from the model, the TCs experienced the maximum intensity. A significant contribution to PV comes from the term where is the potential temperature and p is the pressure. Hence model and ECMWF calculated comparatively higher PV in TCs over the BOB because of the warmer than AS. The model used NCEP FNL reanalysis of six hourly 1 × 1 degree data as input. The results compared with the corresponding values come from the globally scaled ECMWF reanalysis high-resolution 5th Generation (ERA5) hourly data of 0.25° × 0.25°. Therefore, the results from the model may differ slightly from the corresponding values of ECMWF. Hence the results from the model outputs have shown that the WRF model successfully simulated the parameters used to calculate PV.

4.2 Intensification of TC

There are many challenges in the intensity forecasting of TC due to the lack of observations. Therefore to improve the existing forecasting system, meteorologists have been taking numerous measures. The use of the PV technique in the analysis of TC intensity may yield new insights into the NIO. Low pressure at the centre and wind speed around the centre are important parameters to measure the intensity of TC.

Central pressure

The central pressure calculated by the model appeared as though upper PV suppressed the central pressure of the TCs. The increase of the upper tropospheric PV caused a decrease in the central pressure. Such inverse relation was maintained in all the studied events for a particular time (**Figure 2**). This inverse relation continued until the upper PV reached below 3×10^{-6} $m^2s^{-1}KKg^{-1}$. Pressure drop continued in Mekunu over the whole period of model run (**Figure 2**). In Amphan, the pressure drop stopped over the last 24-hour spell even though it had sufficient upper PV and underwent decay. Such behaviour of upper PV in Amphan requires extensive study.

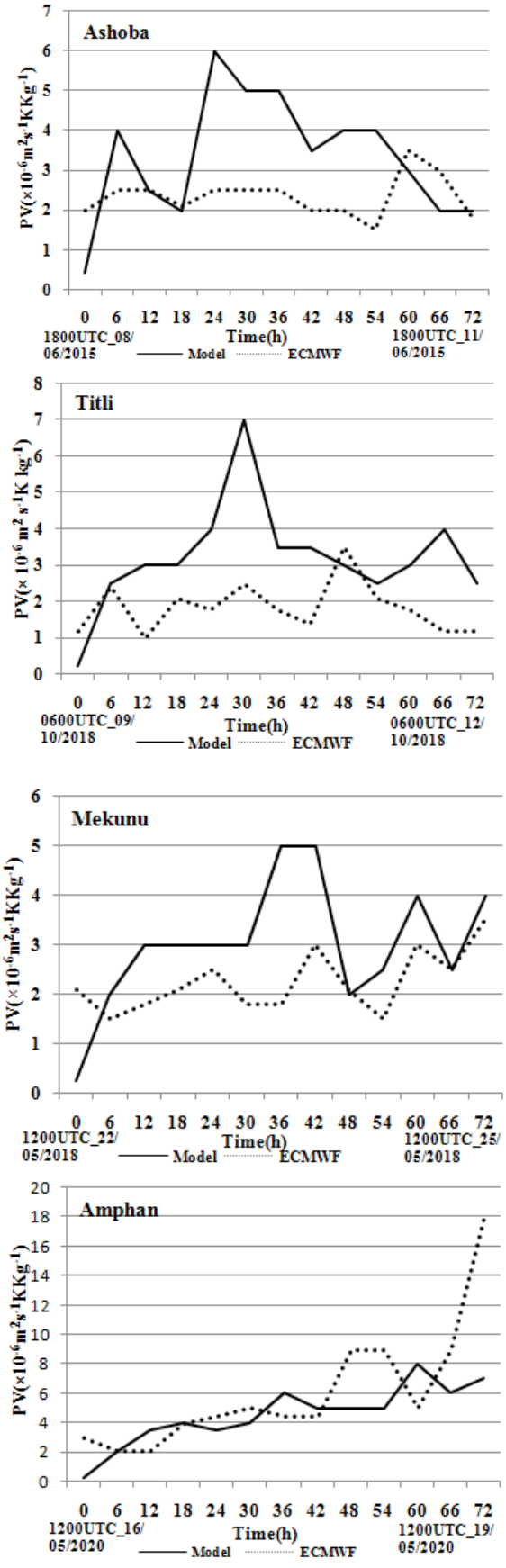

Figure 1. Time evolution of 200 hPa level PV.

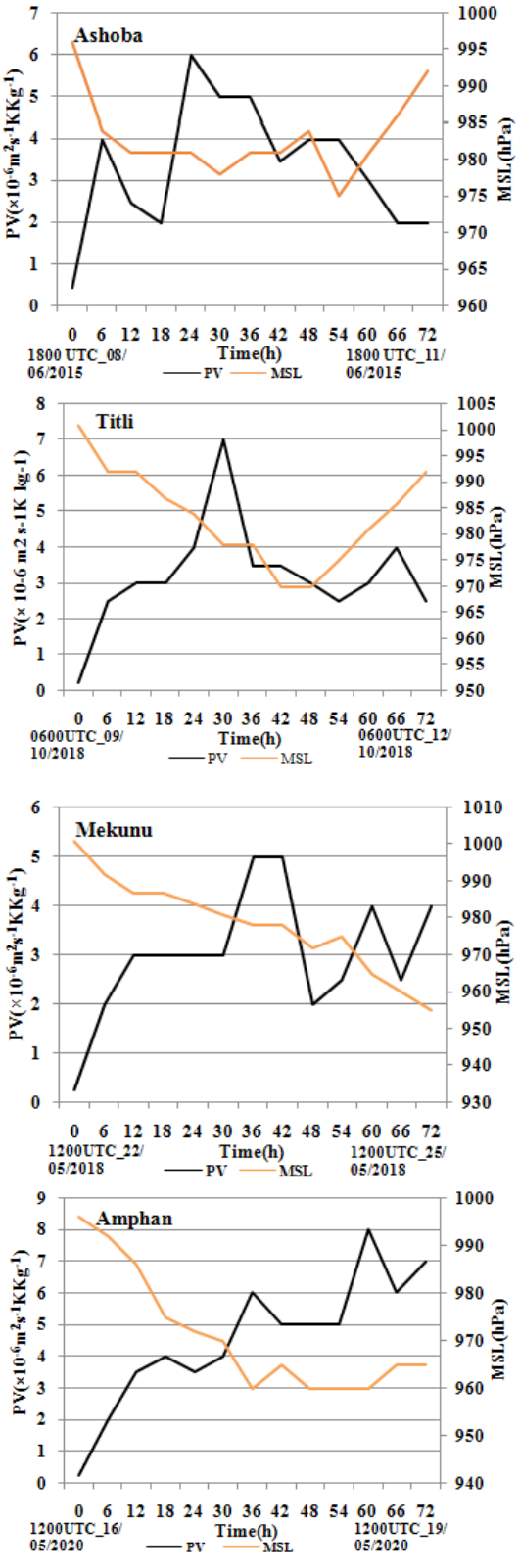

Figure 2. Variation of the model calculated 200 hPa level PV with central pressure.

Wind

Dry and warm conditions are the dominant features of the centre of TC. The most devastating and threatening phenomena exhibited by the eyewall of TC. The interaction between upper PV and low-level wind speed is significant in the eye wall region. The low-level maximum wind speed computed by the model was found closer to that of ECMWF values. The peak values of low-level wind by the model followed the corresponding peak values of ECMWF (**Figure 3**). Comparatively, ECMWF computed wind speeds are of smaller values. The low-level wind speed was found incremental with upper PV over the ocean surface in all the studied events. Almost all of the cyclones we studied found high wind speeds at the peak of the upper PVs (**Figure 4**). Therefore, higher PV favoured the intensification of TCs.

4.3 PV and shear

Wind shear removes the energy in terms of heat and moisture from the TC core. Wind shear causes the TC vortex to tilt away from its base. The high wind shear resists the formation and intensification of TC. Therefore, wind shear is a significant parameter for the genesis and intensification of TC. The wind shear and upper PV exhibited almost identical temporal evolution. The PV line has appeared as though simultaneously it works as a suppressor and exaggerator of the wind shear. That is, it seems as if the upper PV acts as a regulator of the wind shear. In Mekunu, the wind shear didn't exceed the threshold value (12 ms^{-1}) required for the formation and intensification of TC for the whole period of the model run. In Ashoba, Titli and Amphan, the wind shear during the last 12 hours spell of the model run was found negative and above the threshold value. Such characteristics of the wind shear forced the decay of Ashoba, Titli and Amphan though they had sufficient upper PV (**Figure 5**). This relationship between upper PV and wind shear requires further extensive study for accurate forecasting.

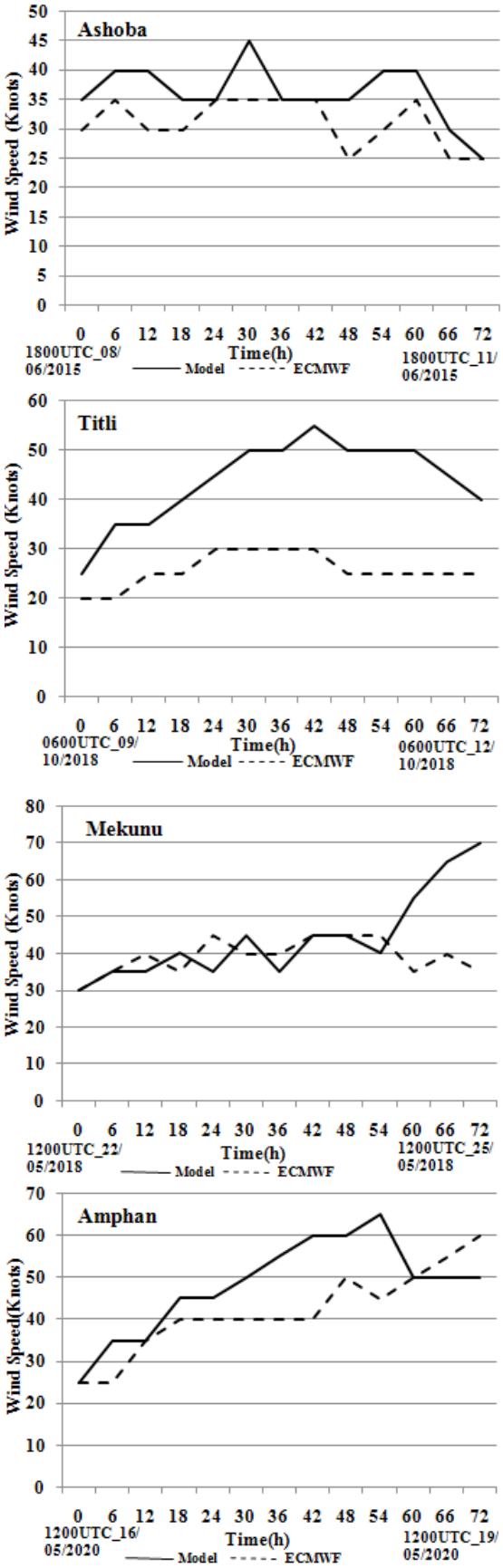

Figure 3. Variation of 850 hPa wind speed with time by model and ECMWF.

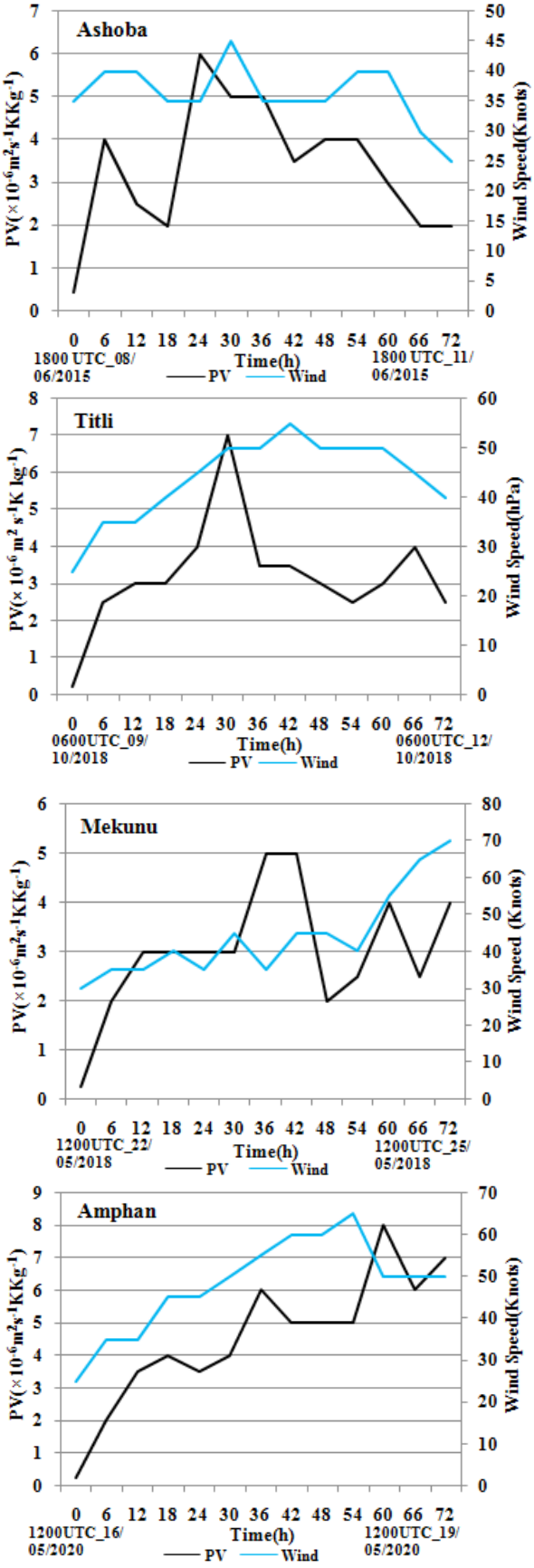

Figure 4. Evolution of 200 hPa level PV and 850 hPa maximum wind speed.

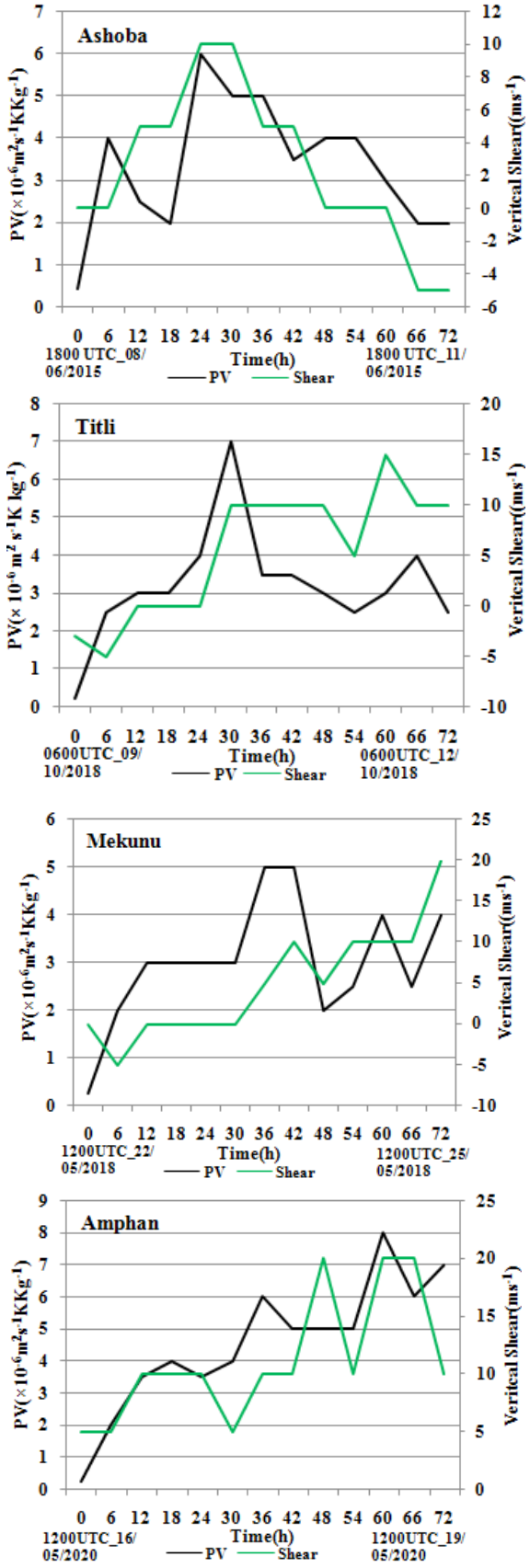

Figure 5. Variation of 200 hPa PV and vertical wind shear with time by model.

4.4 Geopotential height of 500 hPa level

The 500 hPa level in the troposphere has considerable importance for forecasting storms. The wind flow below this level is almost in the same direction. As a result, any event occurring at this level substantially affects the weather below it. Variations in geopotential height at the 500 hPa level affect various atmospheric events at the sea surface. High and low geopotential heights at the said level produce ridges and troughs. Anti-cyclones and cyclones form gradually under these ridges and troughs at sea level. The geopotential heights decrease with the increase of upper PV. The model results show that the upper PV and geopotential heights alternate mutually in opposite trends over the ocean. Acute fall of geopotential height found in Titli, Mekunu and Amphan with the rising of upper PV. Ashoba experienced a slower decline in geopotential height and didn't favour the intensification. The lowering of geopotential height continued over the whole period of the model run of Mekunu and kept up its intensification. A sharp fall of geopotential height found in Titli, Mekunu and Amphan underwent decrying (**Figures 4 and 6**).

5. Concluding remarks

Previous research has shown that upper PV dominates the genesis and intensification of TC. Studies have also shown that upper PV plays a significant role in steering TC's motion. As PV has an implicit effect on tropical cyclone intensification, there is a need for research on the relationship of dynamical parameters with upper PV in the NIO. Fine-scale observational study of PV structure may provide unrevealed insights into TC intensifications. To unearth the role of PV in the structure and intensity change of TC over the NIO is crucial. The following insights are the outcomes of the present study:

1) At least 1 PVU upper PV is required to maintain the intensification of TC.

2) In BOB, upper PV was found higher than that of AS.

3) An increase in upper PV accelerates the pressure drop in the centre of the TC.

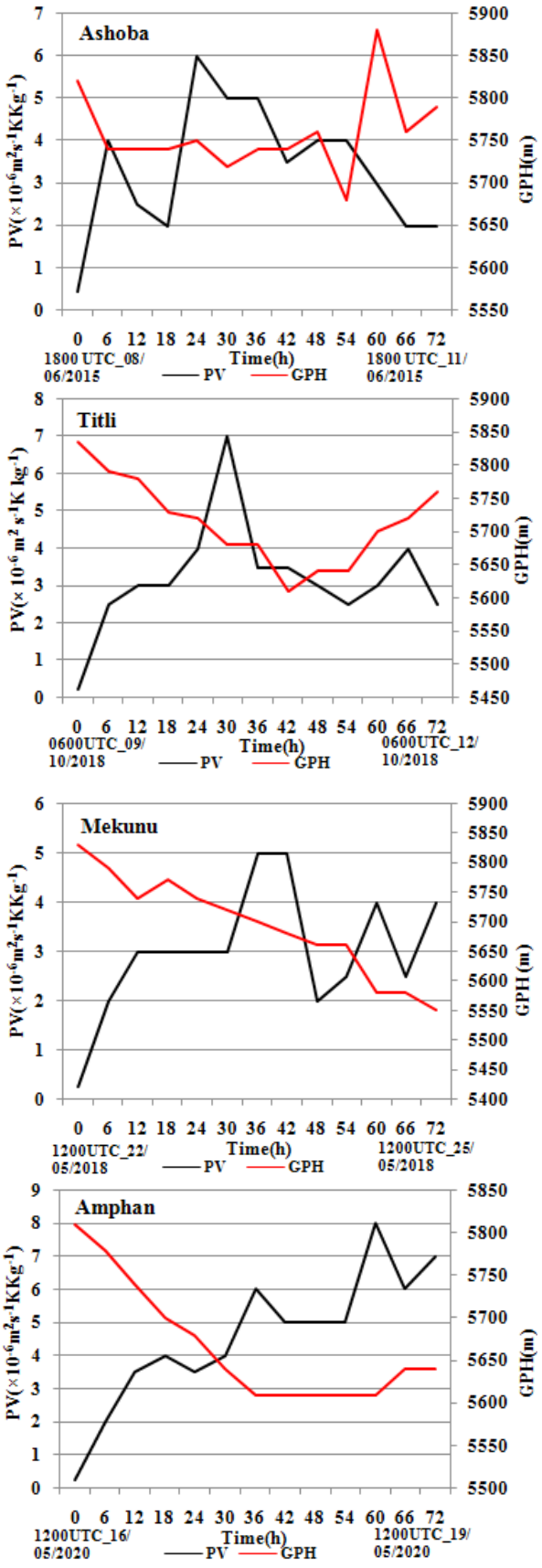

Figure 6. Temporal variation of 200 hPa level PV and 500 hPa level geopotential height in the model.

4) The rise in upper PV favours the low-level wind speed over the ocean.

5) The wind shear and upper PV exhibit almost similar temporal evolution over the ocean.

6) The TCs with negative wind shear and wind shear above the threshold value of 12 m/s couldn't intensify even if they had sufficient upper PV.

7) The upper PV and geopotential heights change in opposite trends.

The results obtained from the present study will play a significant role in forecasting tropical cyclones in the Bay of Bengal basin. Furthermore, considerable attention should pay to the effect of upper PV on atmospheric dynamic and thermodynamic instability.

Author Contributions

A.H.M. Fazla Rabbi (Corresponding author) engaged with the model run, record keeping, data analysis, interpretation and drafting of the manuscripts. Ishtiaque M. Syed and Md. Abdullah Elias Akhter (Co-authors) was involved with designing, providing suggestions and editing the manuscript. M A K Mallik (Co-author) was concerned with reasoning, planning and computing.

Conflict of Interest

There is no conflict of interest among the authors as well as the funder.

Funding

University Grants Commission of Bangladesh financed the research to carry on.

Acknowledgement

The authors acknowledge the financial support from the University Grants Commission of Bangladesh. We express our deep gratitude to the Bangladesh Meteorological Department for giving us extensive technical assistance. We thank National Centres for Environmental Prediction (NCEP) and European Centre for Medium-Range Weather Forecasts(ECMWF) for providing reanalysis data to us.

References

[1] Molinari, J., Skubis, S., Vollaro, D., et al., 1998. Potential vorticity analysis of tropical cyclone intensification. Journal of the Atmospheric Sciences. 55(16), 2632-2644.

[2] Martinez, J., Bell, M.M., Rogers, R.F., et al., 2019. Axisymmetric potential vorticity evolution of Hurricane Patricia (2015). Journal of the Atmospheric Sciences. 76(7), 2043-2063. DOI: https://doi.org/10.1175/JAS-D-18-0373.1

[3] Schubert, W.H., Slocum, C.J., Taft, R.K., 2016. Forced, balanced model of tropical cyclone intensification. Journal of the Meteorological Society of Japan. 94(2), 119-135. DOI: https://doi.org/10.2151/jmsj.2016-007

[4] Wu, C.C., Emanuel, K.A., 1995. Potential vorticity diagnostics of hurricane movement. Part II: Tropical storm Ana (1991) and Hurricane Andrew (1992). Monthly Weather Review. 123(1), 93-109.

[5] Schubert, W.H., Montgomery, M.T., Taft, R.K., et al., 1999. Polygonal eyewalls, asymmetric eye contraction, and potential vorticity mixing in hurricanes. Journal of the Atmospheric Sciences. 56(9), 1197-1223.

[6] Miglietta, M.M., Cerrai, D., Laviola, S., et al., 2017. Potential vorticity patterns in Mediterranean "hurricanes". Geophysical Research Letters. 44(5), 2537-2545. DOI: https://doi.org/10.1002/2017GL072670

[7] Wu, C.C., Wu, S.N., Wei, H.H., et al., 2016. The role of convective heating in tropical cyclone eyewall ring evolution. Journal of the Atmospheric Sciences. 73(1), 319-330. DOI: https://doi.org/10.1175/JAS-D-15-0085.1

[8] Hausman, S.A., Ooyama, K.V., Schubert, W.H., 2006. Potential vorticity structure of simulated hurricanes. Journal of the Atmospheric Sciences. 63(1), 87-108.

[9] May, P.T., Holland, G.J., 1999. The role of potential vorticity generation in tropical cyclone rainbands. Journal of the Atmospheric Sciences. 56(9), 1224-1228.

[10] Schubert, W.H., Alworth, B.T., 1987. Evolution of potential vorticity in tropical cyclones. Quarterly Journal of the Royal Meteorological Society. 113(475), 147-162.

[11] Rozoff, C.M., Kossin, J.P., Schubert, W.H., et al., 2009. Internal control of hurricane intensity variability: The dual nature of potential vorticity mixing. Journal of the Atmospheric Sciences. 66(1), 133-147. DOI: https://doi.org/10.1175/2008JAS2717.1

[12] Möller, J.D., Smith, R.K., 1994. The development of potential vorticity in a hurricane-like vortex. Quarterly Journal of the Royal Meteorological Society. 120(519), 1255-1265.

[13] Yang, B., Wang, Y., Wang, B., 2006. The effect of internally generated inner-core asymmetries on tropical cyclone potential intensity. Journal of the Atmospheric Sciences. 64(4), 1165-1188. DOI: https://doi.org/10.1175/JAS3971.1

[14] Wang, Y., 2008. How do outer spiral rainbands affect tropical cyclone structure and intensity? Journal of the Atmospheric Sciences. 66(5), 1250-1273. DOI: https://doi.org/10.1175/2008JAS2737.1

[15] Deng, D., Davidson, N.E., Hu, L., et al., 2017. Potential vorticity perspective of vortex structure changes of tropical cyclone Bilis (2006) during a heavy rain event following landfall. Monthly Weather Review. 145(5), 1875-1895. DOI: https://doi.org/10.1175/MWR-D-16-0276.1

[16] Judt, F., Chen, S.S., 2010. Convectively generated potential vorticity in rainbands and formation of the secondary eyewall in hurricane Rita of 2005. Journal of the Atmospheric Sciences. 67(11), 3581-3599. DOI: https://doi.org/10.1175/2010JAS3471.1

[17] Yau, M.K., Liu, Y., Zhang, D.L., et al., 2004. A multiscale numerical study of hurricane Andrew (1992). Part VI: Small-scale inner-core structures and wind streaks. Monthly Weather Review. 132(6), 1410-1433.

[18] Jabbar, M.A.R., Hassan, A.S., 2022. Evaluation of geopotential height at 500 hPa with rainfall events: A case study of Iraq. Al-Mustansiriyah Journal of Science. 33(4), 1-8. DOI: http://doi.org/10.23851/mjs.v33i4.1161

[19] Christidis, N., Stott, P.A., 2015. Changes in the geopotential height at 500 hPa under the influence of external climatic forcings. Geophysical Research Letters. 42(24), 10798-10806. DOI: https://doi.org/10.1002/2015GL066669